Usnic acid enantiomers restore cognitive deficits and neurochemical alterations induced by Aβ1−42 in mice

Camila Andre Cazarin [a,*], Ana Paula Dalmagro [a], Ana Elisa Gonçalves [a], Thaise Boeing [a], Luísa Mota da Silva [a], Rogério Corrêa [a], Luiz Carlos Klein-Júnior [a], Bernardo Carlesso Pinto [b], Thaís Savoldi Lorenzett [b], Thales Uchôa da Costa Sobrinho [b], Ângelo de Fátima [c], Tiago Coelho de Assis Lage [d], Sergio Antonio Fernandes [d], Márcia Maria de Souza [a]

[a] Pharmaceutical Sciences Postgraduate Program, Center of Health Sciences, Universidade do Vale do Itajaí, CEP 88302-202, Itajaí, Santa Catarina, Brazil
[b] School of Health Sciences, Universidade do Vale do Itajaí, CEP 88302-202, Itajaí, Santa Catarina, Brazil
[c] Department of Chemistry, Universidade Federal de Minas Gerais, CEP 31270-901, Belo Horizonte, Minas Gerais, Brazil
[d] Department of Chemistry, Universidade Federal de Viçosa, CEP 36570-900, Viçosa, Minas Gerais, Brazil

ARTICLE INFO

ABSTRACT

Alzheimer's disease (AD) is the most prevalent form of dementia with a complex pathophysiology not fully elucidated but with limited pharmacological treatment. The Usnic acid (UA) is a lichen secondary metabolite found in two enantiomeric forms: (R)-$(+)$-UA or (S)-$(-)$-UA, with antioxidant and anti-inflammatory potential. Thus, given the role of neuroinflammation and oxidative injury in the AD, this study aimed to investigate experimentally the cognitive enhancing and anti-neuroinflammatory effects of UA enantiomers. First, the interactions of UA on acetylcholinesterase (AChE) was assessed by molecular docking and its inhibitory capability on AChE was assessed *in vitro*. *In vivo* trials investigated the effects of UA enantiomers in mice exposed to $A\beta_{1-42}$ peptide (400 pmol/mice) intracerebroventricularly (i.c.v.). For this, mice were treated orally during 24 days with (R)-$(+)$-UA or (S)-$(-)$-UA at 25, 50, or 100 mg/kg, vehicle, or donepezil (2 mg/kg). Animals were submitted to the novel object recognized, Morris water maze, and inhibitory-avoidance task to assess the cognitive deficits. Additionally, UA antioxidant capacity and neuroinflammatory biomarkers were measured at the cortex and hippocampus from mice. Our results indicated that UA enantiomers evoked complex-receptor interaction with AChE like galantamine *in silico*. Also, UA enantiomers improved the learning and memory of the animals and in parallel decreased the myeloperoxidase activity and the lipid hydroperoxides (LOOH) on the cortex and hippocampus and reduced the IL-1β levels on the hippocampus. In summary, UA restored the cognitive deficits, as well as the signs of LOOH and neuroinflammation induced by Aβ1−42 administration in mice.

1. Introduction

Alzheimer's disease (AD) is a neurodegenerative disorder that affects approximately 40 million people. Recent estimates show that AD patients can reach over 70 million in 2030 [1]. Although the AD pathogenesis is not fully understood, the amyloid hypothesis is one of the most accepted to explain the events underlying AD's onset and progression [2].

The deposits of extracellular fragments from an erroneous cleavage of the amyloid precursor protein (APP) promoted by β-secretase (BACE1) and ɣ-secretase in C99 APP domain is a pivotal event in the amyloid hypothesis. Subsequently, the amyloidogenic pathway is activated, inducing the release of several *beta*-amyloid fragments (Aβ) with 40–42 amino acid residues into the extracellular space. The $A\beta_{1-42}$ chain is described as a more cytotoxic isoform due to two insoluble amino acids in its structure [3]. In turn, the $A\beta_{1-42}$ aggregation in the central nervous system (CNS) structures triggers oxidative stress, neuroinflammation, and neuronal apoptosis [4]. Furthermore, a process of hyperphosphorylation and abnormal aggregation of a microtubule-associated protein (TAU) forming neurofibrillary tangles (NFT's) occur and has been admitted as an intracellular marker of AD [5].

Clinical evidence observed in AD patients includes the growing

---

degeneration of brain tissue and a pronounced deficiency in acetylcholine (ACh) levels mainly in hippocampus and cortex regions [6]. Is known that ACh is metabolized by acetylcholinesterase (AChE), which converts ACh to choline (Ch) and acetate. Given the Ach deficiency in AD, the cholinesterase inhibitors such as donepezil, rivastigmine, and galantamine are used in the therapy for patients with mild, moderate, or severe AD dementia. In addition to cholinesterase inhibitors, the memantine, a non-competitive *N*-methyl-D-aspartate receptor antagonist and a dopamine agonist, is also approved for use in patients with moderate-to-severe AD [7]. However, both treatment lines are palliative and cannot treat the complexity of events associated with the disease. These drugs also evoked important side effects, which compromise the adherence of the patients to the pharmacological treatment. Thus, the search for new pharmacological targets and agents for the treatment of AD is necessary.

Furthermore, the neuroinflammation has been recognized as a consequence of a primary lesion that leads to glial cells activation, mainly in microglia, in various neuropsychiatric conditions [8]. Indeed, Aβ deposition that occurs in AD promotes the recruitment of activated microglia, releasing high levels of pro-inflammatory mediators such as interleukins (IL)-1β, IL-6 and tumoral necrosis factor (TNF), which in turn also contributes to the more production and accumulation of Aβ [9]. Furthermore, the increased activity of myeloperoxidase (MPO) in activated microglia during the neurodegenerative processes amplify the neuroinflammatory process [4]. In this way, activated microglia plays a key role in the development and advance of neuroinflammation processes related to AD, and the neuroinflammatory process mitigation has been a promising tool for AD therapeutics [10].

Usnic acid (UA) is a secondary lichen metabolite first isolated in 1844 and commonly found in *Alectoria, Cladonia, Usnea, Ramalina, Cetraria,* and *Parmelia* species [11–13]. Briefly, it is presented in two enantiomeric forms (*R*)-(+)- and (*S*)-(-) (Fig. 1) according to the position of a methyl group attached to the chiral carbon 9b, and chemically characterized as a dibenzofuran derivative soluble in ether, acetone, chloroform, ethyl acetate, and dimethyl sulfoxide [12]. Previous studies demonstrated that UA exhibited an anti-inflammatory and antioxidant response in a model of acute lung injury, attenuating MPO levels, and increasing the activity of antioxidant enzymes [14]. Considering this evidence, we can speculate that UA enantiomers may have a desirable potential for the pharmacological treatment of a neurodegenerative disorder related to oxidative stress and neuroinflammation process, such as AD. UA enantiomers also have structural similarities with galantamine, one of the anticholinesterase drugs used in the AD treatment. Therefore, this study aimed to investigate the potential of UA enantiomers in restoring the cognitive deficits, oxidative imbalance, and neuroinflammation process displayed by Aβ$_{1-42}$ in mice and using *in silico* and *in vivo* approaches.

2. Materials and methods

2.1. Molecular docking

The molecular docking tool was employed to predict the binding affinity between UA enantiomers and AChE. In this *in silico* assay, the coupling energy of the UA enantiomers was compared with galantamine due to the structural similarity, and donepezil, the drug used as a positive control in the *in vivo* assays. In line with this, Autodock Vina software was used, in which the ligand behaves a flexible structure [15]. The protein database (RSCB – Protein Data Bank) was retrieved from the structures of the human AChE (PDB 1EVE code). All binders have been developed by the ACD/ChemSketch [16] and underwent subsequent geometric optimization in software Chimera 1.12 [17] using the Amber force package FF14 s. The charges were added using the Gasteiger package. The target receptors were prepared without removing the solvents and amino acids have been correct by the Dunbrank rotamers database. The molecular docking was developed through scripts for virtual screening. After, the docking poses of ligands were observed using Chimera 1.12.

2.2. In vitro inhibitory assay

Inhibition of cholinesterase activity of each UA enantiomer was conduct using the methodology as described by Ellman et al. [18] with some modifications. Tacrine (0.16 μM), galantamine (30 μM), and donepezil (0.4 μM) were used as positive control. Briefly, Wells were filled with 158 μL of Ellman's reagent [0.15 mM final concentration of 5,5′-dithiobis-(2-nitrobenzoic acid) in 0.1 M phosphate buffer pH 7.4], 20 μL of an acetylthiocholine iodide solution (0.33 mM) or S-butyryl thiocholine iodide (0.3 mM), and 2 μL of a solution of the tested compounds solubilized in DMSO. As negative control, only DMSO was used. To start the reaction, 20 μL of an electric eel AChE or serum horse Butyrylcholinesterase (BChE) solution (1 U.I./mL in 0.1 M phosphate buffer pH 7.4, containing human serum albumin at 1 mg/mL) was added. The absorbance at 420 nm was monitored for 10 min (intervals of 60 s between readings) in a microplate reader. Each sample was tested in triplicate, and the percentage of inhibition was determined as follows:

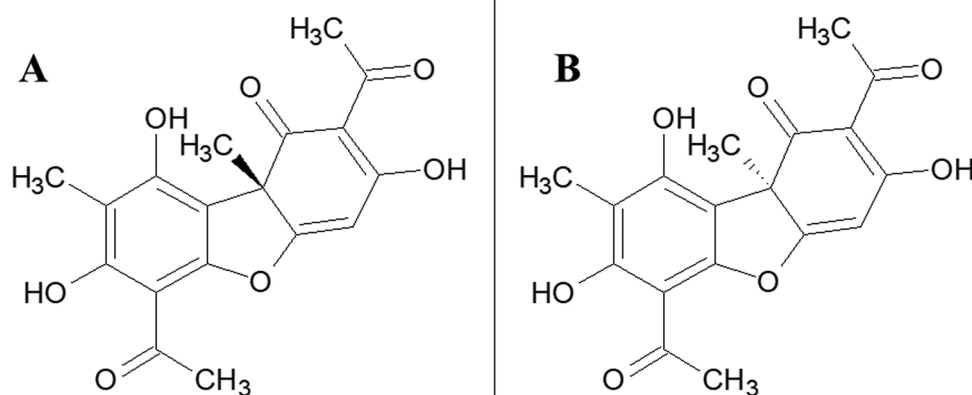Inhibition (%) = [1 − (sample reaction rate/blank reaction rate)] × 100.

Fig. 1. Enantiomeric forms of usnic acid: (A) (*R*)-(+)-UA and (B) (*S*)-(-)-UA. The authors thank ChemSketch.

2.3. Animals and treatments

Pharmacological tests were carried out according to ethical principles of experimental standards, and all protocols were approved by the Ethics Committee for Animal Use (CEUA/UNIVALI – 070/2017). Female swiss mice (25−35 g.) were kept at a temperature of 22 ± 2 °C, with food and water *ad libitum* and light/dark cycle controlled of 12 h (lights on 6:30 am). The animals were divided into ten groups: (1) Naïve; (2) Sham; (3) $A\beta_{1-42}$ plus Vehicle; (4) $A\beta_{1-42}$ plus (R)-(+)-UA 25 mg/kg; (5) $A\beta_{1-42}$ plus (R)-(+)-UA 50 mg/kg; (6) $A\beta_{1-42}$ plus (R)-(+)-UA 100 mg/kg; (7) $A\beta_{1-42}$ plus (S)-(-)-UA 25 mg/kg; (8) $A\beta_{1-42}$ plus (S)-(-)-UA 50 mg/kg; (9) $A\beta_{1-42}$ plus (S)-(-)-UA 100 mg/kg; (10) $A\beta_{1-42}$ plus donepezil 2 mg/kg. The groups Naïve and sham were employed as controls of the procedures. The naive group was formed by animals that did not undergo chemical or surgical intervention. The Sham group (false operated) was formed by animals that underwent the same surgical interventions necessary to dispense the amyloid peptide by intracerebroventricular route but did not receive the peptide. The treatments with vehicle, UA enantiomers or positive control were administered *per oral* (p.o.). The number of animals for each experimental group was approximately 9 mice [19].

2.4. Drugs and reagents

Human $A\beta_{1-42}$ and donepezil were obtained from Sigma Chemicals Co. (USA). Human $A\beta1-42$ was prepared at a concentration of 1 mg/mL, dissolved in sterile 0.1 M phosphate buffered saline (PBS, 137 mM NaCl; 10 mM Na2HPO4; 1.8 mM KH2PO4; 2.7 mM KCl; pH 7.4) and incubated at 37 °C for 4 days [20,21]. The (S)-(-)-UA was isolated from *Cladonia rappii* species collected from Serra do Brigadeiro State Park, located in Araponga, Minas Gerais, Brazil [22]. UA enantiomers, and donepezil solutions were prepared daily with distilled water plus DMSO 2 % before the use.

2.5. Intracerebroventricular (i.c.v.) injection of $A\beta_{1-42}$

The aggregate form of $A\beta_{1-42}$ (400 pmol/mice) was administered by a single i.c.v. injection performed as described earlier [19,23,24] under xylazine plus ketamine anesthesia (10 mg/kg and 80 mg/kg, respectively). After the loss of postural reflexes, local anesthesia was applied into the upper region of the head followed by an incision for removal of tissues and cap display skull. Subsequently, 3 μl of $A\beta_{1-42}$ was injected by i.c.v. route using a 5 μL Hamilton micro syringe coupled to hypodermic needle 0.4 mm. The procedure took place by inserting the needle under the skull of mice according to the coordinates from bregma: 1 mm from the central to a point at cranial
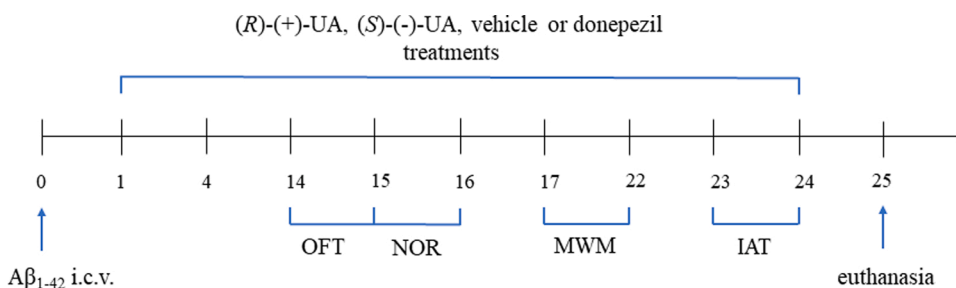
fissures equidistant from each eye, at a distance of between the eyes and the ears and perpendicular to the plane of the skull. After surgery, animals were kept in boxes under lighting 40 W until full recovery and control of hypothermia induced by anesthesia. After, the animals were transferred to housing boxes (6 individuals per box). The application was confirmed using an animal as control where it was injected by i.c.v. route with 2 % Evans blue solution (3 μl), and the brain was dissected to confirm the administration route [25].

The treatment period started twenty-four hours after the recovery of animals and the mice received the treatments for twenty-four days. From the 14th day of treatment, the animals were submitted to the open field test (OFT). The memory was evaluated through novel object recognition (NOR), Morris water maze (MWM), and inhibitory-avoidance test (IAT). The time course of experimental protocol is depicted in Fig. 2.

2.6. Behavioral tests

The animals were acclimatized in a room under low-intensity light in the day of the experiments, for at least 1 h before the procedures. After each tested animal, the apparatus was cleaned with ethanol solution (10 % v/v) and dried to avoid odor impregnation.

2.7. Open field test (OFT)

The locomotor activity of mice was assessed at 14th day after the $A\beta_{1-42}$ administration, through an open field arena which consists of a wooden box measuring $30 \times 30 \times 30$ cm with the floor divided into 9 equal squares, as previously described [26]. The mice could explore the arena freely and the number of squares crossed with all paws (crossing) and the number of vertical posture (exploratory behavioral, rearings) were registered in 6 min sessions [27].

2.8. Novel object recognition (NOR)

To evaluate the recognition memory as well as exploring behavior of mice, the novel object recognition test was used. At the 15th day from the $A\beta_{1-42}$ infusion, the animals were presented to the OFT apparatus with the presence of two identical objects (A + A) with the same color and shape during 10 min (training session/familiarization phase). In the 16th day, one of the objects was replaced with a novel object (object B), which was different in shape and color, and mice were allowed explore the arena and the objects for 10 min (test session). Recognition memory was assessed by comparing the time that the animal spent exploring each object during the test session. The recognition index (RI) was calculated according to the formula $(RI) = B / (B + A)$ where B is the novel object exploration time and A is the familiar object exploration time [28].

Fig. 2. Time course of the experimental protocol. Female swiss mice were administered by intracerebroventricular (i.c.v.) route with $A\beta_{1-42}$ peptide (400 pmol/mice). Pharmacological treatments started 24 h after the infusion, and different groups (n = 9) were treated with vehicle, UA enantiomers (R)-(+)-UA and (S)-(-)-UA at doses 25, 50 and 100 mg/kg (p.o.) or donepezil at 2 mg/kg (p.o.) for 24 days. Mice were submitted to open field test (OFT) at 14th and novel object recognized test (NOR) at 15th and 16th days after the $A\beta_{1-42}$ injection. Training sessions and probe trial of the Morris water maze (MWM) protocol were conducted from the 17th to the 22nd day. Finally, mice were evaluated in the Inhibitory-avoidance test (IAT) on the 24th day. The animals were euthanized 25 days after the peptide administration, and the hippocampus and cortex were dissected for subsequent biochemical analysis.

2.9. Morris Water Maze (MWM)

The Morris water maze, also known as the Morris water navigation task, is a behavioral procedure widely used in behavioral neuroscience to study spatial learning and memory [29]. This apparatus consists of a circular pool (polyethylene tank), 100 cm in diameter and 50 cm tall filled with water, kept at a temperature of 25 °C (±1). The pool floor is divided into four quadrants and numbered clockwise. A circular platform (12 cm in diameter and 25 cm in height) was placed below the water surface, in the center of one quadrant and geometric shapes were fixed around the walls of the pool and on the walls of the room around the pool, allowing the animals to guide themselves and spatially locate the platform. The animals were trained for 5 days (from the 17th to the 21 st day after $A\beta_{1-42}$ administration) to acquire the task at MWM with a daily session. The time spent by each animal to find the platform (escape latency) each day was recorded for analysis. The probe trial was held in the second moment (22th day after administration of the $A\beta_{1-42}$), with the withdrawal of the aquatic maze platform, and the animal had sixty seconds of free-swimming and the time spent in each quadrant was recorded for analysis. The probe trial evaluates the accuracy of spatial learning of the animal represented by the time spent in the quadrant where the platform was located in the training sessions. This analysis is indicative of verifying if the animal used a strategy of spatial orientation to locate the position of the platform in relation to visual clues from the environment [30].

2.10. Inhibitory-avoidance test (IAT)

The inhibitory-avoidance test involves learning an aversive task (training session) and avoiding it in a future context (test session) [31]. The apparatus used for the evaluation of aversive emotional memory of animals is an automated box produced by Insight® (Ribeirão Preto, Brazil). Part of the base of the apparatus has a grid with brass bars of 1 mm in diameter, with 1 cm space. At the training session (a single session), each animal was placed by the platform where was triggered a timer to verify lowering latency. When this occurred, the animal received a shock of 0.4 mA for a period of 2 s. The test session occurred 24 h after the training session, and the animals were submitted to the apparatus with the omission of the shocks. Differences between the step-down latencies from the platform of training and testing sessions considered the memory index [19].

2.11. Tissue preparation and biochemical analysis

Twenty-four hours after the last behavioral test, the animals were euthanized, and their brains were dissected into cortex and hippocampus. These structures were homogenized in potassium phosphate buffer solution 200 mM (pH 6.5) at a dilution ratio equal to 1:3 (w/v) that immediately was used to quantify the levels of reduced glutathione (GSH) [32], lipid hydroperoxides (LOOH) [33] and measurement of cytokines (TNF and IL-1β). The remain homogenate was centrifuged at $9000 \times g$ for twenty minutes at 4 °C to obtain the supernatant which were used to determine the activity of superoxide dismutase (SOD) [34] while the pellet was suspended to determine myeloperoxidase (MPO) activity [35,36]. The protein concentrations were determined by the Bradford method (Bio-Rad, 159 Hercules, CA, USA).

2.11.1. Determination of LOOH and GSH content

The levels of LOOH were determined using the method of ferrous oxidation-xylenol orange 2 (FOX2) as described by Jiang et al. [33]. Briefly, 50 μl of methanol was mixed to 50 μl of homogenate from cortex or hippocampus and centrifuged at $9000 \times g$ for 20 min at 4 °C. The supernatant was added to 4 mM butylated hydroxytoluene, 250 mM $FeSO_4$, 25 mM H_2SO_4, and xylenol orange 100 mM and incubated for 30 min at 25 °C. The absorbance at 560 nm was determined and the results expressed as μmol/mg of tissue using the extinction coefficient of

43.6/M/cm for H_2O_2, cumene hydroperoxide or butyl hydroperoxide.

Further, a portion of homogenate were deproteinized with 12.5 % trichloroacetic acid and centrifuged at $900 \times g$ during 15 min under 4 °C. After, 10 μl of the supernatant was added to 280 μl of 0.4 M TRIS−HCl buffer (pH 8.9) plus 10 μL of 5,5′-dithiobis-2-nitrobenzoic acid at 10 mM. The absorbance at 405 nm was measured after 20 min and the values were interpolated to a standard curve of GSH (1–10 μg/mL) and expressed as μg GSH/g of tissue [32].

2.11.2. Determination of the SOD and MPO activity

The SOD activity was determined as described by Marklund and Marklund [34]. The aliquots of the supernatant from the homogenates were mixed with 1 mM Pyrogallol plus buffer solution composed by 1 mM Tris HCl and 5 mM EDTA (pH 8.5). The reaction was incubated during 20 min and stopped by 1 N HCl addition. After the end reaction, the absorbance at 405 nm and the amount of SOD able to inhibit the oxidation of pyrogallol by 50 %, relative to the control, was defined as one unit of SOD activity. The SOD activity was expressed as U/mg of protein.

To measure the MPO activity, the precipitate from the homogenate was mixed with 80 mM of potassium phosphate buffer (pH 5.4), which contains hexadecylmethylammonium bromide, and centrifuged at $11,000 \times g$ for 20 min at 4 °C. The MPO activity in the presence of hydrogen peroxide and 3,3′, 5,5′-tetramethylbenzidine was determined at 620 nm in the supernatant and expressed in units of optical density (mO.D)/mg of protein [35].

2.11.3. Determination of the TNF and IL-1β levels

The TNF and IL-1β levels were assessed by enzyme-linked immunosorbent assay (ELISA) using mouse cytokine ELISA kits from Invitrogen® (Thermo Fisher Scientific, EUA), according to the manufacturer's instructions. The analytical sensitivity to TNF and IL-1β was 8 pg/mL, as stated by the manufacturer.

2.12. Statistical analyses

The parametric results were expressed as means ± standard error of the means (S.E.M) and statistical significance was obtained by one or two-way analysis of variance (ANOVA), followed by Tukey's test, when applicable. Kruskal-Wallis test followed by Dunn's test was used to evaluate non-parametric results, which was expressed as median ± interquartile ranges. The Kolmogorov-Smirnov normality test was applied to verify the data normality. Moreover, power analysis was performed to determine all sample sizes. Differences were significant when $p < 0.05$, by using the GraphPad Prism version 5.00 for Windows (GraphPad Software, California, USA) program.

3. Results

3.1. Molecular docking

The crystallographic structure of human AChE was obtained with the structure of donepezil in PDB, and for method's validation was used an overlap of donepezil structure designed by ChemSketch with donepezil coupling structure. The similarity of overlapping poses determines the validation method. A coupling energy obtained between the AChE and donepezil was -12 kcal/mol (Fig. 3A). The galanthamine was coupled with the enzyme and given the active sites of molecular interaction. A binding energy -5.7 kcal/mol was obtained for this interaction (Fig. 3B). The (S)-(-)-UA demonstrated an energy-coupling of -6.2 kcal/mol, while (R)-(+)-UA demonstrated an energy-coupling of -6.9 kcal/mol, still active sites have been identified this interaction and it was observed that both enantiomers occupy the same space in AChE that the molecule of donepezil. As the coupling energy of both enantiomers demonstrate similar and the (R)-(+)-enantiomer has obtained a better representative position (Fig. 3C).
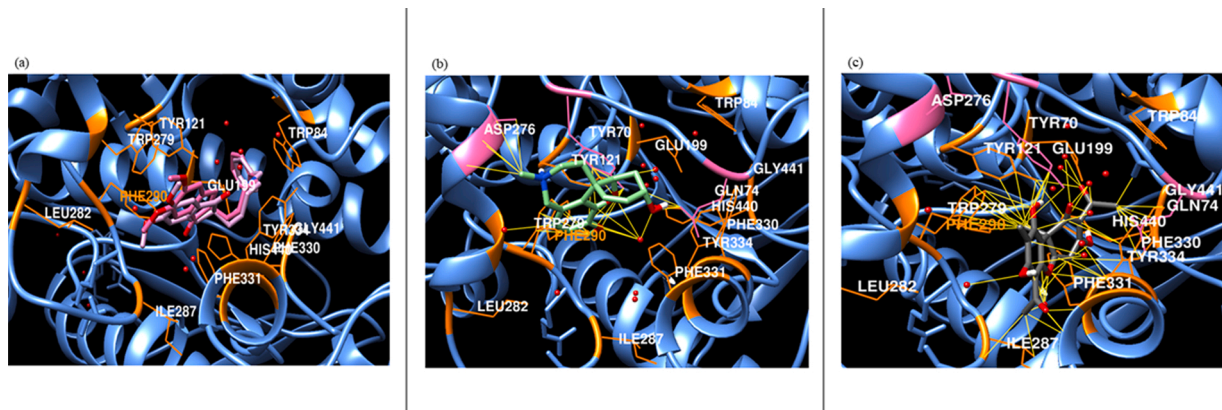
Fig. 3. (A) Overlap of the donepezil structure along with the crystallographic structure, on the structure of the docked donepezil, validating the docking procedure by the similarity of the poses. (B) Interaction of galantamine with the probable peripheral anionic site of AChE. The interactions performed with the amino acids ASP276, GLN 74, TYR 70 and TRP 279. There is still interaction with water molecules, which have a fundamental role in the docking of substrates in this target molecule. (C) Interaction of the (R)-(+)-UA with the catalytic gorge and the internal anionic site in which the interactions with the amino acids are by the type π-stacking. Interactions with water molecules also observed and the space occupied by the usnic acid is like that occupied by the reference drug donepezil.

3.2. UA enantiomers exhibited nootropic effect in memory deficits Aβ$_{1-42}$ induced in mice

One-way ANOVA for NOR performance revealed a difference in recognition index ($F_{(9, 80)} = 4.185$, $p = 0.0002$) Fig. 4A. According to post-hoc analysis, Aβ$_{1-42}$ i.c.v. promoted a decrease of the vehicle group compared to Naïve ($p < 0.001$) and Sham group ($p < 0.01$) i.c.v. Remarkably, the recognition index-impairment promoted by Aβ$_{1-42}$ i.c. v. in the NOR was recovered in the animals that had been treated with UA enantiomers (for (R)-(+)-UA 25 ($p < 0.001$), 50 ($p < 0.01$) and 100 ($p < 0.01$) respectively; (S)-(-)-UA 25 ($p < 0.01$), 50 ($p < 0.01$) and 100 $p < 0.001$) respectively), exhibiting a similar result as donepezil treatment ($p < 0.01$) Fig. 4A. In Fig. S1 of supplementary material, data demonstrate an increase in the discrimination index. ($F_{(9, 80)} = 2.284$, $p = 0.0246$). Furthermore, in this figure, it is possible to access the total exploration time data for two identical objects ($F_{(9, 80)} = 1.951$, $p = 0.0562$) and total exploration time data for familiar plus the novel object ($F_{(9, 80)} = 2.143$, $p = 0.0350$). For MWM probe trial task illustrated in Fig. 4B, one-way ANOVA showed a difference on time spent in training quadrant ($F_{(9, 79)} = 7.652$, $p < 0.0001$). Post-hoc analysis revealed a time decrease at training quadrant permanence of the vehicle group (compared to naïve $p < 0.0001$; sham $p < 0.0001$). In this way, UA enantiomers treatment was able to increase the training quadrant permanence (for (R)-(+)-UA 25 ($p < 0.01$), 50 ($p < 0.05$) and 100 ($p < 0.01$) respectively; (S)-(-)-UA 25 ($p < 0.01$), and 100 $p < 0.01$) respectively), as the same observed in the Donepezil group ($p < 0.0001$). About scape latencies during training sessions data, see Table S1 of supplementary material. Finally, at IAT (Fig. 4C) Aβ$_{1-42}$ promotes a decrease on step-down latency of platform at test session compared to Naïve ($p < 0.0001$) and Sham group ($p < 0.05$) (One-way ANOVA; ($F_{(9, 67)} = 4.743$, $p = 0.0001$). UA enantiomers treatments increased the step-down latency in this session, when compared to vehicle (for (R)-(+)-UA 25 ($p < 0.001$), 50 ($p < 0.001$) and 100 ($p < 0.01$) respectively; (S)-(-)-UA 25 ($p < 0.05$), 50 ($p < 0.05$) and 100 ($p < 0.001$) respectively) as the same observed in the Donepezil group ($p < 0.0001$). Inhibitory-avoidance training session is available on supplementary material as Table S2. To discard locomotor effects due the treatments, mice was evaluated using OFT and the results shown no differences in crossing and rearing number among experimental groups ($p > 0.05$; Table 1).

3.3. Oxidative stress evaluation

As shown in Fig. 5A, one-way ANOVA revealed no difference in SOD activity measured in the cortex ($F_{(9, 49)} = 0.9503$, $p = 0.4916$), but significant alterations among groups when evaluated in hippocampus ($F_{(9, 48)} = 4.546$, $p = 0.0002$). Additionally, post-hoc analysis showed that the SOD activity was attenuated with (R)-(+)-UA treatment at 50 mg/kg ($p < 0.05$) and 100 mg/kg ($p < 0.01$) and (S)-(-)-UA at 100 mg/kg ($p < 0.05$) in hippocampus from mice exposed to Aβ$_{1-42}$ (Fig. 5B). No differences were observed between naïve and sham group ($p > 0.05$).

Regarding the GSH levels, one-way ANOVA indicated no differences in cortex ($F_{(9, 46)} = 1.277$, $p = 0.2750$) (Fig. 5C), but alterations in hippocampus ($F_{(9, 54)} = 8.674$, $p < 0.0001$) (Fig. 5D). Except for (R)-(+)-UA 100 mg/kg ($p < 0.05$ compared with vehicle), the UA treatments were not able to restore GSH levels in the hippocampus region, exhibited by post-hoc analysis (compared with naïve group $p < 0.05$) (Fig. 5D).

As show in Fig. 5E, one-way ANOVA revealed a significant increase in cortical LOOH levels ($F_{(9, 52)}$, $p = 13.72$) after the Aβ$_{1-42}$ i.c.v. administration. Post-hoc analysis demonstrated LOOH increased levels in vehicle or sham group compared to naïve group ($p < 0.05$). Moreover, the treatments with (R)-(+)-UA at 25, 50 and 100 mg/kg ($p < 0.0001$) or (S)-(-)-UA at 25 ($p < 0.0001$), 50 or 100 mg/kg ($p < 0.01$) were able to reduce cortical LOOH levels in mice exposed to Aβ$_{1-42}$, according to post-hoc analysis. At the hippocampus, significant difference also was showed by one-way ANOVA ($F_{(9, 54)}$, $p = 3.771$). The Aβ$_{1-42}$ i.c.v. administration also increased the LOOH levels in the vehicle group compared to naïve group ($p < 0.05$), when analyzed by the post-hoc test. The treatments with (R)-(+)-UA at doses of 25 ($p < 0.01$), 50 ($p < 0.05$) and 100 mg/kg ($p < 0.01$) or (S)-(-)-UA at doses of 25 ($p < 0.01$), 50 ($p < 0.01$) and 100 mg/kg ($p < 0.001$) reversed the increase of hippocampal LOOH in mice.

3.4. Neuroinflammation evaluation

Finally, we investigated the influence of UA treatment on neuro-inflammatory parameters. According to one-way ANOVA, significant differences of MPO activity were showed in cortex (Fig. 6A) ($F_{(9, 50)} = 9.996$, $p < 0.0001$) and hippocampus (Fig. 6B) ($F_{(9, 47)} = 3.044$, $p = 0.0060$) of mice. Regarding the cortical region, post-hoc analysis revealed an increased level of MPO activity promoted by Aβ$_{1-42}$ administration in vehicle group when compared with naïve group ($p < 0.0001$). Interestingly UA enantiomers treatments were able to reverse this increase ($p < 0.0001$) and the same was observed with donepezil administration ($p < 0.0001$). Considering the hippocampal region (Fig. 6B), post-hoc analysis demonstrated that Aβ$_{1-42}$ administration promoted an increase of MPO activity observed in vehicle group
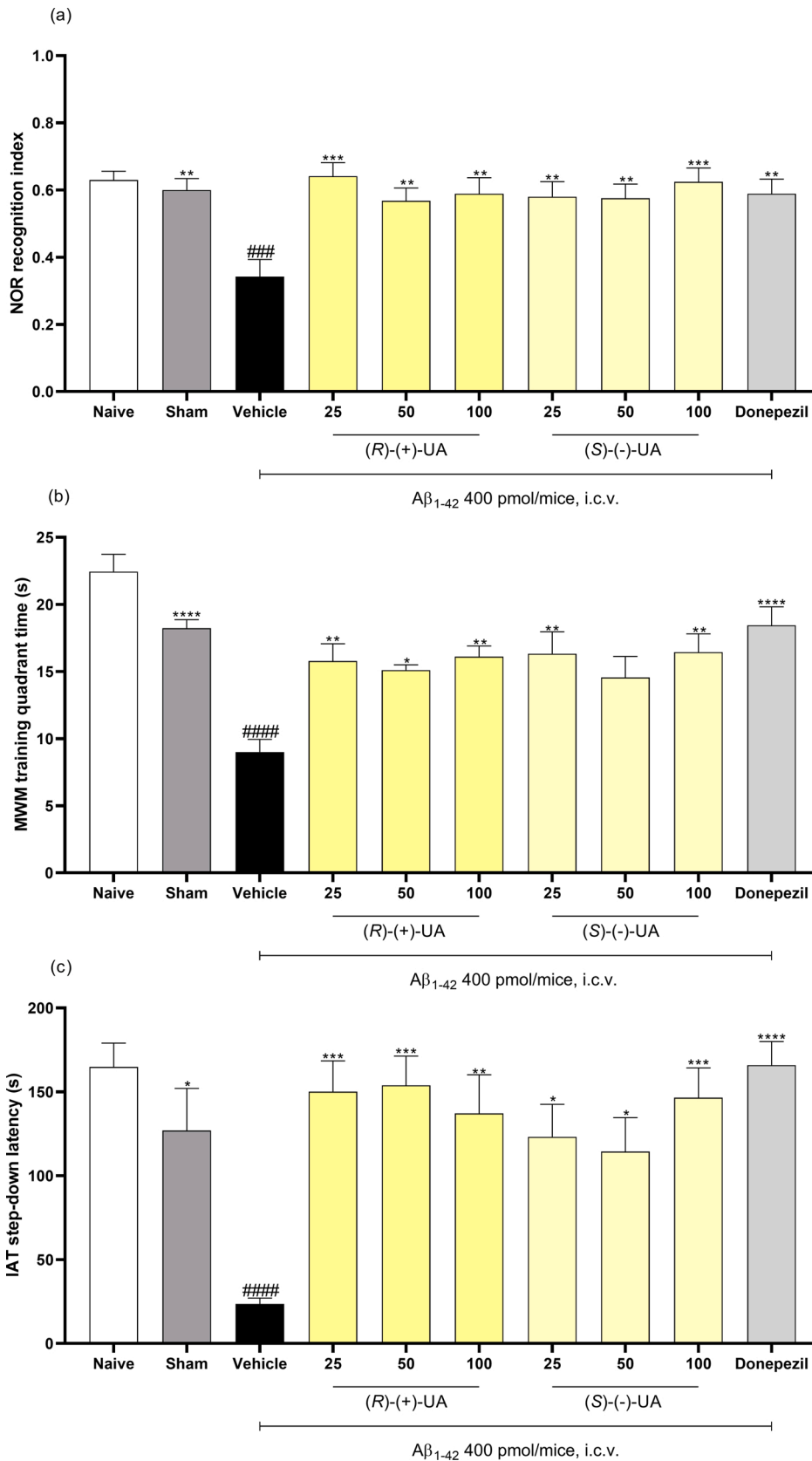
Fig. 4. Behavioral effects of UA enantiomers treatment in mice exposed to Aβ1–42-administration (400 pmol/mice, i.c.v.). Effect of i.c.v. Aβ$_{1-42}$-administration (400 pmol/mice) and UA enantiomers [(R)-(+)-UA and (S)-(-)-UA at doses 25, 50 and 100 mg/kg (p.o.) or donepezil at 100 mg/kg (p.o.)] for 24 days in mice submitted to novel object recognized test (NOR), Morris water maze (MWM), and Inhibitory-avoidance test (IAT). (A) Recognition index of novel object recognized test; (B) MWM probe trial session; (C) IAT test session. Results are represented by mean ± S.E.M. n = 9 per group. Statistical significance was determined by one-way ANOVA followed by Tukey's *post hoc*. **Sham** – group of animals that received no i.c.v. Aβ$_{1-42}$-administration. *p < 0.05; **p < 0.01; ***p < 0.001, and ****p < 0.0001 when compared with Aβ$_{1-42}$ + vehicle group. #p < 0.05; ##p < 0.01; ###p < 0.001, and p < 0.0001 when compared with naïve group.

Table 1
Effect of the treatment of UA enantiomers [(R)-(+)-UA and (S)-(-)-UA)] at doses 25, 50 and 100 mg/kg (p.o.) or donepezil (2 mg/kg, p.o.) for 24 days in mice exposed to $A\beta_{1-42}$-administration (400 pmol/mice, i.c.v.) and submitted to open field test.

	Crossings	Rearings
Naïve	123.7 ± 4.5	57.6 ± 5.1
Sham	127.8 ± 5.4	63.3 ± 4.9
$A\beta_{1-42}$+Vehicle	130.2 ± 8.6	68.7 ± 5.6
$A\beta_{1-42}$+(R)-(+)-UA 25	144.2 ± 10.8	56.1 ± 7.4
$A\beta_{1-42}$+(R)-(+)-UA 50	132.5 ± 8.7	67.8 ± 11.5
$A\beta_{1-42}$+(R)-(+)-UA 100	150.7 ± 11.6	57.8 ± 8.6
$A\beta_{1-42}$+(S)-(-)-UA 25	131.8 ± 5.2	53.6 ± 5.2
$A\beta_{1-42}$+(S)-(-)-UA 50	145.6 ± 8.9	52.0 ± 5.1
$A\beta_{1-42}$+(S)-(-)-UA 100	130.2 ± 4.8	61.2 ± 6.0
$A\beta_{1-42}$+Donepezil	134.8 ± 8.5	64.3 ± 7.8

Values are presented as means $\pm$ S.E.M. (9 animals/group). Statistical significance was determined by one-way ANOVA followed by Tukey's *post hoc* – p > 0.05.

when compared to naïve group (p < 0.01). The same profile of UA enantiomers exposition was observed in this region, since the post-hoc analysis showed that the treatment with (R)-(+)-UA 25, 50 and 100 mg/kg (p < 0.01; p < 0.001; p < 0.01 respectively) attenuated MPO activity, as well (S)-(-)-UA 25, 50 and 100 mg/kg (p < 0.001; p < 0.01; p < 0.01 respectively), and donepezil (p < 0.01). One-way ANOVA showed no difference on IL-1β levels when evaluated in cortical region (F $_{(9, 40)}$ = 2.251, p = 0.0382) (Fig. 6C). Conversely, one-way ANOVA indicated difference in IL-1β levels measured in the hippocampus of mice (F $_{(9, 28)}$ = 7.043, p < 0.0001). Post-hoc analysis showed a significant increase in hippocampal IL-1β levels triggered by the $A\beta_{1-42}$ administration when compared to naïve group (p < 0.01; Fig. 6D). The treatments with (R)-(+)-UA 25, 50 mg/kg (p < 0.05 respectively) and (S)-(-)-UA 25 mg/kg (p < 0.05) elicited a mitigation in this cytokine levels. Interestingly, one-way ANOVA analysis showed no differences in TNF levels measured in cortex (F $_{(9, 40)}$ = 1.721, p = 0.1160) (Fig. 6E) and hippocampus (F $_{(9, 40)}$ = 0.9274, p = 0.5122) (Fig. 6F) of mice after $A\beta_{1-42}$ administration, as shown in Fig. 6E and F.

4. Discussion

This study evaluated the pharmacological potential of two enantiomeric forms of a secondary lichen metabolite – the usnic acid (UA), in a model of neurodegeneration induced by $A\beta_{1-42}$ in mice. Our results indicated that the cognitive deficits of the animals exposed to $A\beta_{1-42}$ and subjected to memory tests were reversed with UA enantiomers treatment, without compromising its locomotor activity. Interestingly, our findings also indicated that the attenuation of oxidative stress and neuroinflammation induced by $A\beta_{1-42}$ in the brain of mice, mainly in the hippocampus, contributed to the UA nootropics effects. To the best of our knowledge, this is the first report addressing a possible anti-Alzheimer property of UA evaluated in an animal model of AD.

Several pharmacological effects have been attributed to UA, such as gastroprotective, immunostimulatory, antiviral, antimicrobial, anti-inflammatory, antiprotozoal, antinociceptive, antioxidant, and anti-tumoral activity [37]. Specifically, the UA antioxidant and anti-inflammatory properties, and the oxidative stress and neuro-inflammation involved in AD pathogenesis directed our attention to evaluating UA effects in an animal model of AD.

Firstly, we opted to check if the UA enantiomers would have AChE inhibitory potential, as occurs with the main drugs used in the current AD treatment [38]. The molecular docking of the enantiomeric forms and their coupling energy in human AChE compared to galantamine and donepezil were performed. This assessment allows us to characterize the molecular behavior in the binding site of a target protein and establishes the molecular interactions that occur through computational methods [39]. Interestingly, the coupling energy of the enantiomers is like that

observed with the galantamine molecule, possibly due to its structural similarity with galantamine. Furthermore, was also found that the site of interaction used by UA enantiomers demonstrated similarities with donepezil structure, which led us to choose this drug as a positive control for *in vivo* tests. Despite its expressive value, predictive modeling certainly has its limitations and for this reason *in vitro* and *in vivo* trials remains necessary to test a hypothesis. In this context, despite of the possible interaction of UA enantiomers and AChE in the same space in AChE that the donepezil, is possible that the changes in the conformational structure of the enzyme promoted by such interaction with UA are not capable of promoting enzymatic inhibition, as verified in the results of the *in vitro* assay.

Subsequently, *in vivo* tests were conducted to study the pharmacological potential of UA as an anti-Alzheimer drug using a widespread model in the literature [19,23,24]. The model of AD induced by a single i.c.v. injection of $A\beta_{1-42}$ in mice resembles the early phases of AD, and it is a useful as an experimental tool for evaluating the neuroinflammation and oxidative stress-induced toxicity [42,43].

In the neurodegenerative process and dementia, as occurs in AD, the hippocampus and afferent neuronal system are primarily engaged, subsequently the diffusion of neurodegeneration in other parts of the brain progresses [44]. To assess memory loss promoted by $A\beta_{1-42}$ i.c.v. infusion in mice, different memory tests were conducted. NOR is a learning and memory test that evaluates the capacity of short-term and long-term memory of animals [45,46]. The administration of Aβ peptide promoted a cognitive deficit in the animals, since the recognition index of vehicle group exposed to $A\beta_{1-42}$ was diminished. In accordance with Whyte et al. [47], the i.c.v. administration of Aβ peptides causes the first memory loss, named habituation, and evokes a greater permanence of mice exploring the environment, instead of interacting with the objects placed in the apparatus. Consequently, the recognition index of NOR will decrease [47]. In this test, the treatment with UA enantiomers at all doses tested was able to revert the cognitive deficit, exhibiting a similar profile to showed by donepezil treated group.

AD patients also have impaired spatial memory since this ability is intrinsically related to the hippocampus, and this is the first structure affected by the events underlying AD pathophysiology [48]. Here, MWM was used to assess the possible impairments in spatial memory of animals subjected to $A\beta_{1-42}$ i.c.v. administration and the effects of treatment with the UA enantiomers. The results demonstrated that animals from Naïve and Sham groups, and those treated with donepezil and UA enantiomers, decreased the time of escape latency of the platform during the training days, which did not occur in animals subjected to $A\beta_{1-42}$ injection and treated with vehicle, corroborating with Chellammal et al. [44]. Regarding the Probe trial of MWM, the animals exposed to $A\beta_{1-42}$ and treated with donepezil, (R)-(+)-UA 25, 50 and 100 mg/kg or (S)-(-)-UA 25 and 100 mg/kg, showed an increase in the time spending in the training quadrant of the apparatus that previously contained the platform. Particularly, these results may suggest that the treatments were able to reverse spatial memory deficits evoked by the peptide injection.

The IAT and NOR are commonly used for assessing memory of short or long-duration in rodents, respectively [49]. Regarding IAT, the innate reaction of animals is to avoid the punishment triggered by an electric shock, resulting in a possible reduction of that behavior when the stimulus will be repeated. Considering this aversive stimulus, the learning process occurs because animals instinctively seek to avoid these aversive situations, therefore the avoidance response is simply an answer to escape with reduced latency [49–51]. Previously studies [52] reported that the $A\beta_{1-42}$ infusion promotes a decrease in step-down latency, corroborating with our finding. Noteworthy, the animals exposed to $A\beta_{1-42}$ injection and treated with the UA enantiomers in all doses tested, as well the donepezil-treated group, demonstrated similar behavior to Naïve and Sham groups in IAT. Importantly, UA enantiomers could reverse the cognitive deficits evaluated in three behavioral tests of memory.
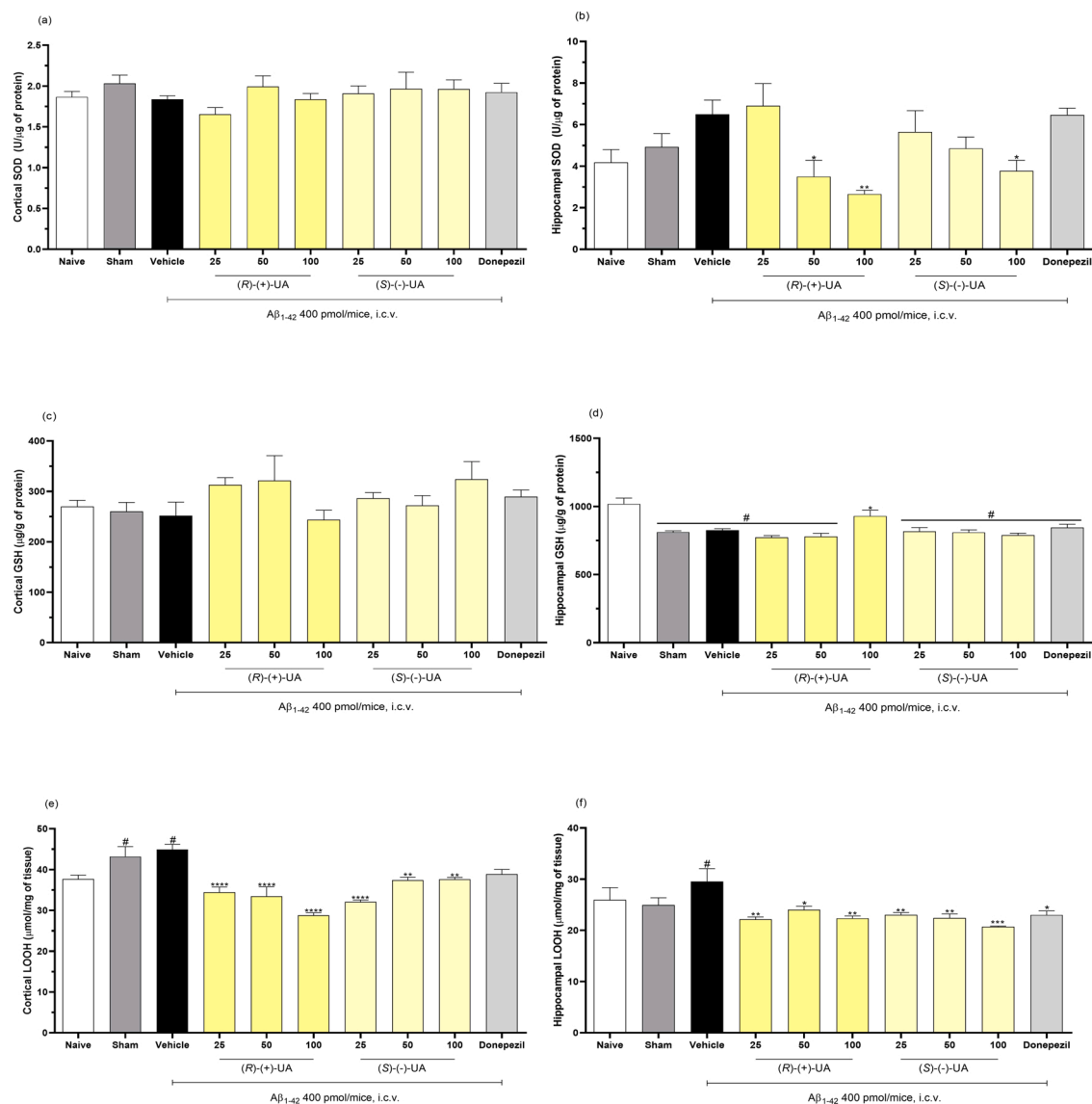
Fig. 5. Antioxidant effects of UA enantiomers in cortex and hippocampus of mice exposed to Aβ1–42-administration (400 pmol/mice, i.c.v.). Effect of i.c.v. Aβ$_{1-42}$-administration (400 pmol/mice) and UA enantiomers ((*R*)-(+)-UA and (*S*)-(-)-UA) at doses 25, 50 and 100 mg/kg (p.o.) or donepezil at 2 mg/kg (p.o.) for 24 days in mice. N = 8-10. *Sham group:* animals did not receive i.c.v. Aβ$_{1-42}$-administration. Panels show the influence of the treatments in the SOD activity in cortex (A) and hippocampus (B), GSH (panels C and D, respectively), and LOOH levels (panels E and F). Results are represented by mean ± S.E.M. n = 9 per group. Statistical significance was determined by one-way ANOVA followed by Tukey's *post hoc*. *p < 0.05; **p < 0.01; ***p < 0.001, and ****p < 0.0001 when compared with Aβ$_{1-42}$ + vehicle group. #p < 0.05; ##p < 0.01; ###p < 0.001, and p < 0.0001 when compared with naïve group.

Despite the results discussed to this point, it is known that the UA possess toxicity potential, mainly in liver and kidney [53]. However, is important emphasize that UA enantiomers still restores cognitive deficits even at the lowest dose tested, that is 25 mg/kg, and that the previous experimental reports about the toxicological potential of UA in mice were described to doses equal to or greater than 50 mg/kg by oral route [54–56]. Moreover, the interest of scientific community about the effects of UA on neurodegenerative diseases has been growing. Lee et al. (2020) [57] evaluated the anti-inflammatory effects of UA against MPTP-induced mouse model of Parkinson's disease. Shi et al. (2019) [58] also confirmed the inhibitory effects of a compound derived from UA on the aggregation of full-length 2N4R tau protein by a heparin-induced mechanism, as well as the anti-inflammatory activity of this compound and sodium usnate in lipopolysaccharide (LPS)-stimulated mouse microglia BV2 cells and its protective effects against okadaic acid-induced memory impairment in rats.

Oxidative stress has been associated with all aspects of AD

pathogenesis and is closely related to the formation of pathological features in AD [59]. AD patients exhibit increased oxidative damage, such as lipid peroxidation, reactive carbonyl and nucleic acid oxidation in their neurons, and the abovementioned oxidative markers are readily apparent in the fragile neurons of AD patients, but not obvious in other diseases, indicating that oxidative stress response occurs earlier than other markers [60]. In fact, obvious oxidative stress can be observed in each phase of AD and this oxidative injury increase with the disease progression [60]. As a hallmark of AD, Aβ is responsible for spatial memory deficit and cognitive dysfunction [45], which in turn can be elicited by oxidative injury due to the accumulation of aberrant amyloidogenic fragment of APP [61]. The *in vitro* antioxidant potential of UA had already been reported [40,41], us encouraged to investigate the effects of UA enantiomers in front of the oxidative damage during the neurodegeneration process experienced by mice exposed to i.c.v. infusion of Aβ$_{1-42}$.

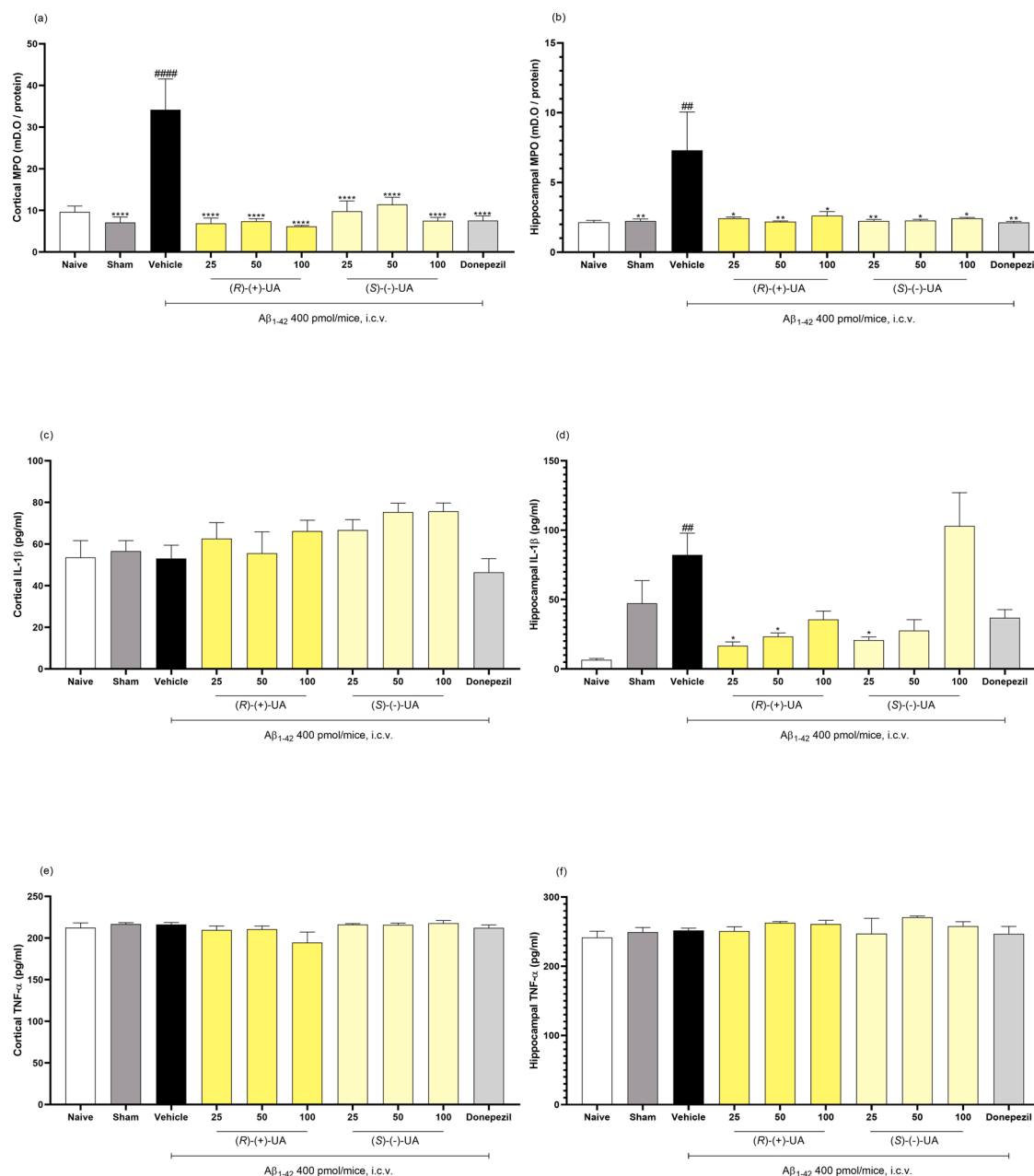Enzymatic antioxidants are the first line of defense against oxygen

Fig. 6. Modulation of inflammatory markers trigger by UA enantiomers in cortex and hippocampus of mice exposed to Aβ1–42-administration (400 pmol/mice, i.c.v.). Effect of i.c.v. Aβ$_{1-42}$-administration (400 pmol/mice) and UA enantiomers ((R)-(+)-UA and (S)-(-)-UA) at doses 25, 50 and 100 mg/kg (p.o.) or donepezil at 2 mg/kg (p.o.) for 24 days in mice. N = 8-10. *Sham group:* animals did not receive i.c.v. Aβ$_{1-42}$-administration. Panels show the results of MPO activity in cortex (A) and hippocampus (B), besides the level of interleukin-1β (panels C and D, respectively) and TNF-α (panels E and F) in both structures. Results are represented by mean ± S.E.M. n = 9 per group. Statistical significance was determined by one-way ANOVA followed by Tukey's *post hoc*. *p < 0.05; **p < 0.01; ***p < 0.001, and ****p < 0.0001 when compared with Aβ$_{1-42}$ + vehicle group. #p < 0.05; ##p < 0.01; ###p < 0.001, and p < 0.0001 when compared with naïve group.

reactive species. The main antioxidant enzymes are superoxide dismutase (SOD), catalase, and glutathione peroxidase (GPx) [61]. Although the role of SOD in the AD remains contradictory, some authors describe the increase of its activity as an AD marker [62], especially in regions of the cortex, hippocampus, and cerebellum from these patients. The increased SOD activity was found in the hippocampus from the vehicle group can be possibly explained by the largest generation of superoxide anion during the neurodegenerative process, which constantly activates the SOD in this susceptible brain region. Interestingly, the treatment with donepezil were unable to avoided this increase in the hippocampus; but the SOD activity was decreased in the hippocampus from animals treated with (R)-(+)-UA (50 or 100 mg/kg) and

(S)-(-)-UA (100 mg/kg). Given that the UA displays a potent scavenger activity against several radicals, including 1,1-diphenyl-2-picrylhydrazyl (DPPH·, IC$_{50}$: 49.50 μg/mL), N,N-dimethyl-p-phenylenediamine (DMPD·$^+$, IC$_{50}$: 33.00 μg/mL), superoxide anion (O$_2^{·-}$, IC$_{50}$: 18.68 μg/mL), and 2,2'-azino-bis(3-ethylbenzthiazoline-6-sulfonic acid) (ABTS·$^+$, IC$_{50}$: 10.41 μg/mL) [63] is possible infer that a direct antioxidant action can mitigate the radical production, including the O$_2^{·-}$, which in turn can reduce the SOD activity due reduction in substrate bioavailability.

GSH is a cofactor of the glutathione peroxidase (GPx) in the reduction of H$_2$O$_2$ into H$_2$O [64]. During the neurodegenerative process in humans or in animal models, GSH levels are decreased while its oxidized

form, the GSSG, are increased [65,66]. In the results from hippocampus, the levels of GSH were diminished after i.c.v. infusion of $A\beta_{1-42}$, like obtained by Koh et al. [64] and Souza et al. [23]. However, the treatment with donepezil or the enantiomers was not able to avoid the GSH depletion, suggesting that glutathione system is not influenced by the administration of the UA enantiomers or that the compounds increased the activity of GPx (which in turn requires GSH as a cofactor during its antioxidant action). In agreement, previous reports [67] also had no difference in the GSH levels in animals submitted to neurodegenerative condition induced by streptozotocin and treated with donepezil when compared to the vehicle group. It has already been demonstrated that donepezil exerts distinct age-related effects on the cell-mediated immune responses through selective modulation of antioxidant enzyme activities and intracellular targets that may influence the therapeutic efficacy of these drugs in neurodegenerative diseases. Donepezil had differential effects on the SOD and catalase activity but increased the activities of GPx and GST [68]. Besides, is possible that the surgical procedure can promote the depletion of this non-enzymatic resource because the sham groups experienced similar levels to found on vehicle group and decreased levels in relation to naïve group.

Previous studies shown that $A\beta_{1-42}$ toxicity is mediated by the damage of cell membranes by free radical species [69] and has been shown that the $A\beta_{1-42}$ is able to promote lipid peroxidation from your solubility in lipid bilayer [70]. In this study, it was verified that i.c.v. administration of $A\beta_{1-42}$ peptide increased the LOOH levels both in the hippocampus and cortex of mice, which is consistent with results from Gunn et al. [71]. In the cortex and hippocampus, the treatment with UA enantiomers were able to attenuate LOOH levels, confirming that the reduction in oxidative damage in these brain regions can mediate the beneficial cognitive effects displayed by these compounds.

$A\beta$ peptides can activate the microglia and promotes the release of pro-inflammatory cytokines such as IL-1β and TNF, contributing to neuronal loss [72]. In the brain, active microglia are responsible for increased activity of MPO, where is implicated in catalyzing the formation of hypochlorous acid, a highly pro-oxidant; therefore, MPO is an important biomarker of neuroinflammatory processes at neurodegenerative diseases [73]. Indeed, studies conducted in humans have already demonstrated that the MPO levels are significantly higher in patients diagnosed with AD when compared to healthy [74]. Here, the $A\beta_{1-42}$ infusion promoted increased levels of MPO activity in both cortex and hippocampus, corroborating with Chen et al. [75], which showed this increase as an indicator of activated microglial cells after $A\beta_{1-42}$ infusion in rabbits; as well the results obtained by Gellhaar et al. [73] investigating the brain of rodents. Interestingly, the treatment with the UA enantiomers in all the dosages used in this study reduced the MPO activity in the cortex and hippocampus of the animals, suggesting reducing in the neuroinflammation process.

The presence of cytokines, such as TNF, can exacerbate $A\beta$ deposits and develop tauopathies [72]. Also, TNF levels are high in CSF and plasma of patients with AD [76]. In accordance with Schmid et al. [77], the data presented here, the i.c.v. infusion of $A\beta_{1-42}$ did not increase levels of this cytokine as well were not reported differences using treatment with UA enantiomers. It is reported that there is an increase in serum levels of IL-1β in AD patients [78]. Furthermore, the present study found that the infusion of i.c.v. $A\beta_{1-42}$ promotes an increase in the IL-1β content, corroborating with Garcez et al. [79]. In contrast, this increase was reversed by treatment with (R)-(+)-UA 25 and 50 mg/kg or (S)-(-)-UA enantiomers at a dose of 25 mg/kg.

As described in our methodology, the oxidative and inflammatory parameters of our study were accessed 25 days after the injection of the $A\beta_{1-42}$ infusion and indicate the persistence of such changes in a longer time than has generally has been accessed in the literature [77,80]. At first, Alzheimer's disease typically destroys neurons and their connections in parts of the brain involved in memory, including the entorhinal cortex and hippocampus and later affects areas in the cerebral cortex responsible for language, reasoning, and social behavior. In accordance,

some differences in inflammatory and oxidative parameters also were found in hippocampus and cortex in our results, similarly to [81], indicating that the hippocampus of rodents is more susceptible to changes promoted by $A\beta_{1-42}$ infusion. Moreover, oxidative damage in the hippocampus is evident in the preclinical stages of AD [82]. Indeed, the hippocampus is commonly regarded as the initiation site of neuronal loss or damage in AD, spreading to the cortex and eventually affecting the entire brain [83].

In accordance with the conclusions of Lee et al. (2020) [57], our results also suggest that the mechanism in which UA enantiomers ameliorate memory performance and alleviate cognitive deficits promoted by $A\beta_{1-42}$ i.c.v. can be related, at least in part, to the attenuation of the neuroinflammation process. In addition, an important issue about the UA enantiomers and its pharmacological potential to treat neurodegenerative disorder is its lower polarity. The UA is lipophilic in both neutral and anionic forms due its β-triketone groups [84] which can favor the passage through biological membranes. In addition, the molecular properties study of UA on basis of "Lipinski's rule of five" using the Molinspiration® server describes that this compound satisfy theoretical parameters required to be a promising drug candidate (360.09 u, log P = 2.4, 8 acceptors of hydrogen, 2 atom donor of hydrogen) [85]. These physicochemical characteristics can be useful to propose that UA is able to pass the blood-brain barrier and exercise activities in the central nervous system. In addition to its lipophilicity, UA is a weak acid (pka = 4.4) and its transport in the blood to brain may be mediated by an organic anion transporter, however further studies are needed to clarify this field.

5. Conclusions

To summarize, the obtained data demonstrate that the treatment with the two UA enantiomeric improved the learning and memory of the mice exposed to $A\beta_{1-42}$ - infusion, which was achieved in OFT, NOR, MWM, and IAT. Is possible infer that this effect is related, at least in part, by the attenuation of the lipoperoxides accumulation on the brain and the neuroinflammation induced by Aβ1–42- exposed mice. Therefore, this study provided evidence regarding the potential of UA enantiomers in restoring cognitive deficits and modulating oxidative/inflammatory cascades, which commonly is associated with AD. However, further studies are crucial, mainly regarding the mechanism of action and approaches to minimize the toxicity related to these compounds.

Declaration of Competing Interest

The authors declare that they have no known competing financial interests or personal relationships that could have appeared to influence the work reported in this paper.

Acknowledgements

Appendix A. Supplementary data

Supplementary material related to this article can be found, in the online version, at doi:https://doi.org/10.1016/j.bbr.2020.112945.

References

[1] E. McDade, R.J. Bateman, Stop Alzheimer's before it starts, Nature 547 (7662) (2017) 153–155, https://doi.org/10.1038/547153a.
[2] A. de Falco, D.S. Cukierman, R.A. Hauser-Davis, N.A. Rey, Doença de Alzheimer: hipóteses etiológicas e perspectivas de tratamento, Quim. Nova 39 (1) (2016) 63–80, https://doi.org/10.5935/0100-4042.20150152.

[3] E. Tönnies, E. Trushina, Oxidative stress, synaptic dysfunction and Alzheimer's disease, J. Alzheimer's Dis. 57 (4) (2017) 1105–1121, https://doi.org/10.3233/JAD-161088.

[4] Z. Cai, M.D. Hussain, L.J. Yan, Microglia, neuroinflammation and beta-amyloid protein in Alzheimer's disease, Int. J. Neurosci. 124 (5) (2014) 307–321, https://doi.org/10.3109/00207454.2013.833510.

[5] Y. Gao, L. Tan, J.T. Yu, L. Tan, TAU in Alzheimer's disease: mechanisms and therapeutic strategies, Curr. Alzheimer Res. 15 (3) (2018) 283–300, https://doi.org/10.2174/1567205014666170417111859.

[6] T.H. Ferreira-Vieira, I.M. Guimarães, F.R. Silva, F.M. Ribeiro, Alzheimer's disease: targeting the cholinergic system, Curr. Neuropharmacol. 14 (1) (2016) 101–115, https://doi.org/10.2174/1570159x13666150716165726.

[7] J. Weller, A. Budson, Current understanding of Alzheimer's disease diagnosis and treatment, F1000Res. 7 (2016) Rev-1161, https://doi.org/10.12688/f1000research.14506.1.

[8] F. Regen, J. Hellmann-Regen, E. Costantini, M. Reale, Neuroinflammation and Alzheimer's disease: implications for microglial activation, Curr. Alzheimer Res. 14 (11) (2017) 1140–1148, https://doi.org/10.2174/1567205014666170203141717.

[9] E.C. Stamouli, A.M. Politis, Pro-inflammatory cytokines in Alzheimer's disease, Psychiatriki. 27 (4) (2016) 264–275, https://doi.org/10.22365/jpsych.2016.274.264.

[10] H. Sarlus, M.T. Heneka, Microglia in Alzheimer's disease, J. Cli. Invest. 127 (9) (2017) 3240–3249, https://doi.org/10.1172/JCI90606.

[11] M. Cocchietto, N. Skert, P.L. Nimis, A review on usnic acid, an interesting natural compound, Naturwissenschaften 89 (4) (2002) 137–149, https://doi.org/10.1007/s00114-002-0305-3.

[12] K. Ingólfsdóttir, Usnic acid, Phytochemistry 61 (7) (2002) 729–736, https://doi.org/10.1016/s0031-9422(02)00383-00387.

[13] K. Muller, Pharmaceutically relevant metabolites from lichens, Appl. Microbiol. Biotechnol. 56 (1–2) (2001) 9–16, https://doi.org/10.1007/s002530100684.

[14] Z.Q. Su, Z.Z. Mo, J.B. Liao, X.X. Feng, Y.Z. Liang, X. Zang, Y.H. Liu, X.Y. Chen, Z. W. Chen, Z.R. Su, X.P. Lai, Usnic acid protects LPS-induced acute lung injury in mice through attenuating inflammatory responses and oxidative stress, Int. Immunopharmacol. 22 (2) (2014) 371–378, https://doi.org/10.1016/j.intimp.2014.06.043.

[15] O. Trott, A.J. Olson, Software news and update Autodock Vina: improving the speed and accuracy of Docking with a new scoring function, efficient optimization and multithreading, J. Comput. Chem. 31 (2) (2010) 455–461, https://doi.org/10.1002/jcc.21334.

[16] ACD, I. A. C. D. Acd/Chemsketch elucidator version 15.01.2015.

[17] E.F. Pettersen, T.D. Goddard, G.S.C.C.C. Huang, D.M. Greenblatt, E.C. Meng, T. E. Ferrerin, Uscf chimera: a visualization system for exploratory research and analysis, J. Comput. Chem. 25 (13) (2004) 1605–1612, https://doi.org/10.1002/jcc.20084.

[18] G.L. Ellman, D.K. Courtney, V. Andres Jr., R.M. Featherstone, A new and rapid colorimetric determination of acetylcholinesterase activity, Biochem. Pharmacol. 7 (2) (1961) 88–95, https://doi.org/10.1016/0006-2952(61)90145-9.

[19] S.K. Amoah, M.T. Dalla Vecchia, B. Pedrini, G.L. Carnhelutti, A.E. Gonçalves, D. A. Dos Santos, M.W. Biavatti, M.M. De Souza, Inhibitory effect of sesquiterpene lactones and the sesquiterpene alcohol aromadendrane-4β,10α-diol on memory impairment in a mouse model of Alzheimer, Eur. J. Pharmacol. 769 (2015) 195–202, https://doi.org/10.1016/j.ejphar.2015.11.018.

[20] C.J. Pike, D. Burdick, A.J. Walencewicz, G.G. Glabe, C.W. Cotman, Neurodegeneration induced by beta-amyloid peptides *in vitro*: the role of peptide assembly state, J. Neurosci. 13 (4) (1993) 1676–1687. PMID: 8463843.

[21] S. Delobette, A. Privat, T. Maurice, In vitro aggregation facilities beta-amyloid peptide (25–35) induced amnesia in the rat, Eur. J. Pharmacol. 319 (1) (1997) 1–4, https://doi.org/10.1016/s0014-2999(96)00922-3.

[22] T.C.A. Lage, T.M.S. Maciel, Y.C.C. Mota, F. Sisto, J.R. Sabino, J.C.C. Santos, I. M. Figueiredo, C. Masia, A. de Fátima, S.A. Fernandes, L.V. Modolo, *In vitro* inhibition of *Helicobacter pylori* and interaction studies of lichen natural products with jack bean urease, New J. Chem. 42 (7) (2018) 5356–5366, https://doi.org/10.1039/C8NJ00072G.

[23] A.C.G. De Souza, C.L. Gonçalves, V. De Souza, J.M. Hartwig, M. Farina, R. D. Prediger, Agmatine attenuates depressive-like behavior and hippocampal oxidative stress following amyloid β1-40 administration in mice, Behav. Brain Res. 353 (2018) 51–56, https://doi.org/10.1016/j.bbr.2018.06.032.

[24] R.D. Prediger, L.F. Jeferson, P. Pandolfo, R. Medeiros, F.S. Duarte, G. Di Giunta, C. P. Figueiredo, M. Farina, J.B. Calixto, R.N. Takahashi, A.L. Dafre, Differential susceptibility following β-amyloid peptide-(1–42) administration in C57BL/6 and Swiss albino mice: evidence for a dissociation between cognitive deficits and the glutathione system response, Behav. Brain Res. 177 (2) (2007) 205–213, https://doi.org/10.1016/j.bbr.2006.11.032.

[25] A. Manaenko, H. Chen, J. Kammer, J.H. Zhang, J. Tang, Comparison Evans blue injection routes: intravenous vs. intraperitoneal for measurement of blood-brain barrier in a mice hemorrhage model, J. Neurosci. Methods 195 (2) (2011) 206–210, https://doi.org/10.1016/j.jneumeth.2010.12.013.

[26] A.L. Rodrigues, J.B. Rocha, C.F. Mello, D.O. Souza, Effect of perinatal lead exposure on rat behaviour in open-field and two-way avoidance tasks, Pharmacol. Toxicol. 79 (3) (1996) 150–156, https://doi.org/10.1111/j.1600-0773.1996.tb00259.x.

[27] A.E. Gonçalves, C. Büerger, S.K.S. Amoah, R. Tolardo, M.W. Biavatti, M.M. De-Souza, The antidepressant-like effect of *Hedyosmum brasiliense* and its sesquiterpene lactone, podoandin in mice: evidence for the involvement of adrenergic, dopaminergic and serotonergic systems, Eur. J. Pharmacol. 674 (2–3) (2012) 307–314, https://doi.org/10.1016/j.ejphar.2011.11.009.

[28] S.J. Cohen, R.W. Stackman Jr, Assessing rodent hippocampal involvement in the novel object recognition task: a review, Behav. Brain Res. 285 (2015) 105–117, https://doi.org/10.1016/j.bbr.2014.08.002.

[29] R.G. Morris, Developments of a water-maze procedure for studying spatial learning in the rat, J. Neurosci. Meth. 11 (1) (1984) 47–60, https://doi.org/10.1016/0165-0270(84)90007-4.

[30] A. Blockland, E. Geraerts, M. Been, A detailed analysis of rats' spatial memory in a probe trial of a Morris task, Behav. Brain Res. 154 (1) (2004) 71–75, https://doi.org/10.1016/j.bbr.2004.01.022.

[31] I. Izquierdo, D.M. Barros, T.M. Souza, M.M. De-Souza, L.A. Izquierdo, J.H. Medina, Mechanisms for memory types differ, Nature 393 (6686) (1998) 635–636, https://doi.org/10.1038/31371.

[32] J. Sedlak, R.H. Lindsay, Estimation of total protein-bound, and nonprotein sulfhydryl groups in tissue with Ellman's reagent, Anal. Biochem. 25 (1968) 192–205, https://doi.org/10.1016/0003-2697(68)90092-4.

[33] Y. Jiang, A. Lee, J. Chen, M. Cadene, B.T. Chait, R. Mackinnon, Crystal structure and mechanism of a calcium-gated potassium channel, Nature 417 (2002) 515–522, https://doi.org/10.1038/417515a.

[34] S. Marklund, G. Marklund, Involvement of the superoxide anion radical in the autoxidation of pyrogallol and a convenient assay for superoxide dismutase, Eur. J. Biochem. 47 (3) (1974) 469–474, https://doi.org/10.1111/j.1432-1033.1974.tb03714.x.

[35] P.P. Bradley, D.A. Priebat, R.D. Christensen, G. Rothstein, Measurement of cutaneous inflammation: estimation of neutrophil content with an enzyme marker, I Invest Dermatol. 78 (3) (1982) 206–209, https://doi.org/10.1111/1523-1747.ep12506462.

[36] M.M. Bradford, A rapid and sensitive method for the quantitation óf microgram quantities of protein utilizing the principle of protein-dye binding, Anal. Biochem. 72 (1–2) (1976) 248–254, https://doi.org/10.1016/0003-2697(76)90527-3.

[37] A.A. Araújo, M.G. de Melo, T.K. Rabelo, P.S. Nunes, S.L. Santos, M.R. Serafini, M. R. Santos, L.J. Quintans-Júnior, D.P. Gelain, Review of the biological properties and toxicity of usnic acid, Nat. Prod. Res. 29 (23) (2015) 2167–2180, https://doi.org/10.1080/14786419.2015.1007455.

[38] A. Atri, Current and future treatments in Alzheimer's disease, Semin. Neurol. 39 (2) (2019) 227–240, https://doi.org/10.1055/s-0039-1678581.

[39] E.A. Lohning, M.S. Levonis, B. Williams-Noonan, S.S. Schweiker, A practical guide to molecular docking and homology modelling for medicinal chemists, Curr. Top. Med. Chem. 17 (18) (2017) 2023–2040, https://doi.org/10.2174/1568026617666170130110827.

[40] R.G. Reddy, L. Veeraval, S. Maitra, M. Chollet-Krugler, S. Tomasi, F.L. Dévéhat, J. Boustie, S. Chakravarty, Lichen-derived compounds show potential for central nervous system therapeutics, Phytomedicine 23 (12) (2016) 1527–1534, https://doi.org/10.1016/j.phymed.2016.08.010.

[41] K.C. Cetin, İ. Gülçin, Anticholinergic and antioxidant activities of usnic acid-an activity-structure insight, Toxicol. Rep. 6 (2019) 1273–1280, https://doi.org/10.1016/j.toxrep.2019.11.003.

[42] X. Wu, Y.G. Lv, Y.F. Du, F. Chen, M.N. Reed, M. Hu, V. Suppiramaniam, S.S. Tang, H. Hong, Neuroprotective effects of INT-777 against Aβ1-42-induced cognitive impairment, neuroinflammation, apoptosis, and synaptic dysfunction in mice, Brain Behav. Immun. 73 (2018) 533–545, https://doi.org/10.1016/j.bbi.2018.06.018.

[43] A. Ahmad, H.Y. Park, H. Badshah, S.U. Rehman, M.O. Kim, Neuroprotective effect of fisetin against amyloid-beta-induced cognitive/synaptic dysfunction, neuroinflammation, and neurodegeneration in adult mice, Mol. Neurobiol. 54 (3) (2017) 2269–2285, https://doi.org/10.1007/s12035-016-9795-4.

[44] H.S.J. Chellammal, V. Alagarsamy, D. Ramachandran, S.B. Gummadi, M. M. Manan, N.R. Yellu, Neuroprotective effects of 1'δ-1'-acetoxyeugenol acetate on Aβ25-35 induced cognitive dysfunction in mice, Biomed. Pharmacother. 109 (2019) 1454–1461, https://doi.org/10.1016/j.biopha.2018.10.189.

[45] L.M. Lueptow, Novel object recognition test for the investigation of learning and memory in mice, J. Vis. Exp. 126 (2017), https://doi.org/10.3791/55718.

[46] J.J. Richler, J.B. Wilmer, I. Gauthier, General object recognition is specific: evidence from novel and familiar objects, Cognition 166 (2017) 42–55, https://doi.org/10.1016/j.cognition.2017.05.019.

[47] L.S. Whyte, K.M. Hemsley, A.A. Lau, S. Hassiotis, T. Saito, T.C. Saido, J. J. Hopwood, T.J. Sargeant, Reduction in open field activity in the absence of memory deficits in the APPNL-G-F knock-in mouse model of Alzheimer's disease, Behav. Brain Res. 336 (2018) 177–181, https://doi.org/10.1016/j.bbr.2017.09.006.

[48] Y. Takei, Age-dependent decline in neurogenesis of the hippocampus and extracellular nucleotides, Hum. Cell 32 (2) (2019) 88–94, https://doi.org/10.1007/s13577-019-00241-9.

[49] L.A. Izquierdo, D.M. Barros, M.R. Vianna, A. Coitinho, T. deDavid e Silva, H. Choi, B. Moletta, J.H. Medina, I. Izquierdo, Molecular pharmacological dissection of short- and long-term memory, Cell. Mol. Neurobiol. 22 (3) (2002) 269–287, https://doi.org/10.1023/A:1020715800956.

[50] I. Izquierdo, C.R. Furini, J.C. Myskiw, Fear memory, Physiol. Rev. 96 (2) (2016) 695–750, https://doi.org/10.1152/physrev.00018.2015.

[51] M.P. García-Pardo, J.E. De la Rubia Ortí, M.A. Aguilar Calpe, Differential effects of MDMA and cocaine on inhibitory avoidance and object recognition tests in rodents, Neurobiol. Learn. Mem. 146 (2017) 1–11, https://doi.org/10.1016/j.nlm.2017.10.013.

[52] M.L. Garcez, F. Mina, T. Bellettini-Santos, A.P. da Luz, G.L. Schiavo, J.M. C. Macieski, E.B. Medeiros, A.O. Marques, N.Q. Magnus, J. Budni, The involvement of NLR3 on the effects of minocycline in an AD like pathology induced by beta-

amyloid oligomers administered to mice, Mol. Neurobiol. 56 (4) (2019) 2606–2617, https://doi.org/10.1007/s12035-018-1211-9.

[53] L. Guo, Q. Shi, J.L. Fang, N. Mei, A.A. Ali, S.M. Lewis, J.E.A. Leakey, V.H. Frankos, Review of usnic acid and Usnea barbata toxicity, J. Environ. Sci. Health C Environ. Carcinog. Ecotoxicol. Rev. 26 (4) (2008) 317–338, https://doi.org/10.1080/10590500802533392.

[54] I. Prokopiev, G. Filippova, E. Filippov, I. Voronov, I. Sleptsov, A. Zhanataev, Genotoxicity of (+)- and (-)-usnic acid in mice, Mutat. Res. Genet. Toxicol. Environ. Mutagen. 839 (2019) 36–39, https://doi.org/10.1016/j.mrgentox.2019.01.010.

[55] H.D.A. Araújo, J.G. Silva-Júnior, J.R.S. Oliveira, M.H.M.L. Ribeiro, M.C.B. Martins, M.A.C. Bezerra, A.L. Aires, M.C.P.A. Albuquerques, M.R. Melo-Júnior, N.T.P. Filho, E.C. Pereira, D.J.R. Silva, J.V. dos Anjos, E.P.S. Falcão, N.H. Silva, V.L.M. Lima, Usnic acid potassium salt: evaluation of the acute toxicity and antinociceptive effect in murine model, Molecules 24 (11) (2019) 2042, https://doi.org/10.3390/molecules24112042.

[56] A.M. al-Bekairi, S. Qureshi, M.A. Chaudhry, D.R. Krishna, A.H. Shah, Mitodepressive, clastogenic and biochemical effects of (+)-usnic acid in mice, J. Ethnopharmacol. 33 (3) (1991) 217–220, https://doi.org/10.1016/0378-8741 (91)90079-S.

[57] S. Lee, Y. Lee, S. Ha, H.Y. Chung, H. Kim, J.S. Hur, J. Lee, Anti-inflammatory effects of usnic acid in an MPTP-induced mouse model of Parkinson's disease, Brain Res. 1739 (2020), 146642, https://doi.org/10.1016/j.brainres.2019.146642.

[58] C.J. Shi, W. Peng, J.H. Zhao, H.L. Yang, L.L. Qu, C. Wang, L.Y. Kong, X.B. Wang, Usnic acid derivatives as tau-aggregation and neuroinflammation inhibitors, Eur. J. Med. Chem. 187 (2019) 111961, https://doi.org/10.1016/j.ejmech.2019.111961.

[59] W.J. Huang, X. Zhang, W.W. Chei, Role of oxidative stress in Alzheimer's disease, Biomed. Rep. 4 (5) (2016) 519–522, https://doi.org/10.3892/br.2016.630.

[60] D.A. Butterfield, Perspectives on oxidative stress in Alzheimer's disease and predictions of future research emphases, J. Alzheimers Dis. 64 (s1) (2018) S469–S479, https://doi.org/10.3233/JAD-179912.

[61] M.T. Islam, Oxidative stress and mitochondrial dysfunction-linked neurodegenerative disorders, Neurol. Res. 39 (1) (2017) 78–82, https://doi.org/10.1080/01616412.2016.1251711.

[62] T. Ma, C.A. Hoeffer, H. Wong, C.A. Massad, P. Zhou, C. Iadecola, M.P. Murphy, R. G. Pautler, E. Klann, Amyloid β-induced impairments in hippocampal synaptic plasticity are rescued by decreasing mitochondrial superoxide, J. Neurosci. 31 (15) (2011) 5589–5595, https://doi.org/10.1523/JNEUROSCI.6566-10.2011.

[63] K.C. Cakmak, I. Gunçin, Anticholinergic and antioxidant activities of usnic acid-an activity-structure insight, Toxicol. Rep. 6 (2019) 1273–1280, https://doi.org/10.1016/j.toxrep.2019.11.003.

[64] E.J. Koh, K.J. Kim, J.H. Song, J. Choi, H.Y. Lee, D.H. Kang, H.J. Heo, B.Y. Lee, *Spirulina maxima* extract ameliorates learning and memory impairments vi inhibiting GSK-3β phosphorylation induced by intracerebroventricular injection of amyloid β $_{1-42}$ in mice, Int. J. Mol. Sci. 18 (11) (2017) E2401, https://doi.org/10.3390/ijms18112401.

[65] L. Balasz, M. Leon, Evidence of an oxidative challenge in the Alzheimer's brain, Neurochem. Res. 19 (9) (1994) 1131–1137, https://doi.org/10.1007/bf00965146.

[66] V. Calabrese, R. Sultana, G. Scapagnini, E. Guagliano, M. Sapienza, R. Bella, J. Kanski, G. Pennisi, C. Mancuso, A.M. Stella, D.A. Butterfield, Nitrosative stress, cellular stress response, and thiol homeostasis in patients with Alzheimer's disease, Antioxid. Redox Signal. 8 (11–12) (2006) 1975–1986, https://doi.org/10.1089/ars.2006.8.1975.

[67] G. Saxena, S.P. Singh, R. Agrawal, C. Nath, Donepezil and Tacrine on oxidative stress in intracerebral streptozotocin-induced model of dementia in mice, Eur. J. Pharmacol. 581 (3) (2008) 283–289, https://doi.org/10.1016/j.ejphar.2007.12.009.

[68] H.P. Priyanka, R.V. Singh, M. Mishra, S. ThyagaRajan, Diverse age-related effects of *Bacopa monnieri* and donepezil *in vitro* on cytokine production, antioxidant enzyme activities, and intracellular targets in splenocytes of F344 male rats, Int. Immunopharmacol. 15 (2) (2013) 260–274, https://doi.org/10.1016/j.intimp.2012.11.018.

[69] C. Ricci, M. Maccarini, P. Falus, F. Librizzi, M.R. Mangione, O. Moran, M.G. Ortore, R. Schweins, S. Vilasi, R. Carrotta, Amyloid β-peptides interactions with membranes: can chaperones change the fate? J. Phys. Chem. B 123 (3) (2018) 631–638, https://doi.org/10.1021/acs.jpcb.8b11719.

[70] Z.H. Guo, M.P. Mattson, In vivo 2-deoxyglucose administration preserves glucose and glutamate transport and mitochondrial function in cortical synaptic terminals after exposure to amyloid beta-peptide and iron: evidence for a stress response, Exp. Neurol. 166 (1) (2000) 173–179, https://doi.org/10.1006/exnr.2000.7497.

[71] A.P. Gunn, B.X. Wong, T. Johanssen, J.C. Griffith, C.L. Masters, A.I. Bush, K. J. Barnhan, J.A. Duce, R.A. Cherny, Amyloid-β peptide Aβ3pE-42 induces lipid peroxidation, membrane permeabilization and calcium influx in neurons, J. Biol. Chem. 291 (2) (2016) 6134–6145, https://doi.org/10.1074/jbc.M115.655183.

[72] D.V. Hansen, J.E. Hanson, M. Sheng, Microglia in Alzheimer's disease, J. Cell Biol. 217 (2) (2018) 459–472, https://doi.org/10.1083/jcb.201709069.

[73] S. Gellhaar, D. Sunnemark, H. Eriksson, L. Olson, D. Galter, Myeloperoxidase-immunoreactive cells are significantly increased in brain areas affected by neurodegeneration in Parkinson's and Alzheimer's disease, Cell Tissue Res. 369 (3) (2017) 445–454, https://doi.org/10.1007/s00441-017-2626-8.

[74] S. Tzikas, D. Schlak, K. Sopova, A. Gatsiou, D. Stakos, K. Stamatelopoulos, K. Stellos, C. Laske, Increased myeloperoxydase plasma levels in patients with Alzheimer's disease, J. Alzheimer Dis. 39 (3) (2014) 557–564, https://doi.org/10.3233/JAD-131469.

[75] Y. Chen, T. Wang, K.A. Rogers, B.K. Rutt, J.A. Ronald, Close association of myeloperoxidase producing activated microglia with amyloid plaques in hypercholesterolemic rabbits, J. Alzheimer Dis. 67 (4) (2019) 1221–1234, https://doi.org/10.3233/JAD-180714.

[76] J.O. Ekert, R.L. Gould, G. Reynolds, R.J. Howard, TNF alpha inhibitors in Alzheimer's disease: a systematic review, Int. J. Geriatr. Psychiatry 33 (5) (2018) 688–694, https://doi.org/10.1002/gps.4871.

[77] S. Schmid, B. Jungwirth, V. Gehlert, M. Blobner, G. Schneider, S. Kratzer, K. Kellermann, G. Rammes, Intracerebroventricular injection of beta-amyloid in mice is associated with long-term cognitive impairment in the modified hole-board test, Behav. Brain Res. 324 (2017) 15–20, https://doi.org/10.1016/j.bbr.2017.02.007.

[78] E. Dursun, D. Gezen-Ak, H. Hanagasi, B. Bilgiç, E. Lohmann, S. Ertan, İ.L. Atasoy, M. Alaylıoğlu, Ö.S. Araz, B. Önal, A. Gündüz, H. Apaydın, G. Kızıltan, T. Ulutin, H. Gürvit, S. Yılmazer, The interleukin 1 alpha, interleukin 1 beta, interleukin 6 and alpha-2-macroglobulin serum levels in patients with early or late onset Alzheimer's disease, mild cognitive impairment or Parkinson's disease, J. Neuroimmunol. 283 (2015) 50–57, https://doi.org/10.1016/j.jneuroim.2015.04.014.

[79] M.L. Garcez, F. Mina, T. Bellettini-Santos, F.G. Carneiro, A.P. Luz, G.L. Schiavo, M. S. Andrighetti, M.G. Scheid, R.P. Bolfe, J. Budni, Minocycline reduces inflammatory parameters in the brain structures and serum and reverses memory impairment caused by the administration of amyloid beta 1-42 in mice, Prog. Neuropsychopharmacol. Biol. Psychiatry 77 (2017) 23–31, https://doi.org/10.1016/j.pnpbp.2017.03.010.

[80] W. Bai, M. Xia, T. Liu, X. Tian, Aβ1-42-induced dysfunction in synchronized gamma oscillation during working memory, Behav. Brain Res. 307 (2016) 112–119, https://doi.org/10.1016/j.bbr.2016.04.003.

[81] X. Mao, Z. Liao, L. Guo, X. Xuo, B. Wu, M. Xu, X. Zhao, K. Bi, Y. Jia, Schisandrin C ameliorates learning and memory deficits by aβ1-42 -induced oxidative stress and neurotoxicity in mice, Phytother. Res. 29 (9) (2015) 1373–1380, https://doi.org/10.1002/ptr.5390.

[82] M.A. Lovell, S.S. Soman, M.A. Bradley, Oxidatively modified nucleic acids in preclinical Alzheimer's disease (PCAD) brain, Mech. Ageing Dev. 132 (8-9) (2011) 443–448, https://doi.org/10.1016/j.mad.2011.08.003.

[83] K. Gosche, J. Mortimer, C.D. Smith, W.R. Markesbery, D.A. Snowdown, Hippocampal volume as an index of Alzheimer neuropathology: findings from the Nun study, Neurology 58 (10) (2002) 1476–1482, https://doi.org/10.1212/WNL.58.10.1476.

[84] A.N. Abo-Khatwa, A.A. Al-Robai, D.A. Al-Jawhari, Lichen acids as uncouplers of oxidative phosphorylation of mouse-liver mitochondria, Nat. Toxins 4 (2) (1996) 96–102.

[85] M.F. Khan, S.A. Nabila, R.B. Rashid, M.S. Rahman, A.A. Chowdhury, M.A. Rashid, In silico molecular docking studies of lichen metabolites against cyclooxygenase-2 enzyme, Bangl. J. Pharmacol. 18 (2) (2015) 90–96, https://doi.org/10.3329/bpj.v18i2.24304.